Journal of Sound and Vibration (1994) **170**(3), 397–409

RESPONSE OF A PERIODICALLY DRIVEN IMPACT OSCILLATOR

W. FANG AND J. A. WICKERT

Department of Mechanical Engineering, Carnegie Mellon University, Pittsburgh, Pennsylvania 15213, *U.S.A.*

(*Received* 7 *May* 1992, *and in final form* 17 *August* 1992)

The response of a single-degree-of-freedom oscillator that can impact a surface with prescribed harmonic motion is investigated through experimental and numerical means. The test apparatus consisted of a stainless steel cantilever beam that could collide with a voice coil shaker which was driven at a specified frequency and amplitude. By collocating the contact and measurement points at a particular location near the free end of the beam, the response was dominated by the beam's fundamental mode. Response time records, frequency spectra and state space trajectories that were measured are compared to those predicted by a non-linear recurrence relation for the oscillator's state from one impact to the next. As borne out by non-dimensionalization of the model, the amplitude of response at a given frequency of excitation is proportional to the amplitude of the surface's motion, notwithstanding the non-linearity of the impact process. On the other hand, the qualitative character of the oscillator's response depends strongly on the frequency of the surface's motion. As the excitation frequency is increased gradually over a range equalling several times the oscillator's natural frequency, the response exhibits a recurring pattern of resonance, period-doubling bifurcation, and irregular non-periodic motion.

1. INTRODUCTION

A variety of mechanical systems can exhibit vibration with intermittent impact, including gear trains with backlash, mechanisms with excessive joint clearance, and such reciprocating machinery as punch presses. Collision between two bodies involves relatively large forces that are generated over a short time interval, and this results in material deformation, recovery and the generation of heat and sound. Impact can be described in the simplest context by the highly empirical coefficient of restitution, which is defined as the ratio of the contact force's restoration and deformation impulses. Alternatively, when compression at the place of contact can be regarded as occurring nearly statically and reversibly, the contact process can be modelled by Hertz's theory of impact. Frequency dependent corrections which account for the radiation of energy into the colliding bodies are available [1]. In each case, however, the contact process is strongly non-linear, being approximated in the former model by a one-sided displacement constraint and an instantaneous change in velocity, and in the latter one by a stiffening spring.

In the light of their non-linear character, impact systems can exhibit interesting dynamic behavior. A prototypical problem in this area is the motion of a concentrated mass that collides with an oscillating surface. Between collisions, the particle is in free flight under gravity. For the case in which the amplitude of the surface's motion is small compared to the excursion of the particle, Holmes [2] derived a difference equation that maps the state of the particle from one impact to the next. There, the state of the system was defined as the time of impact and the velocity of the particle immediately afterwards. In addition

to harmonic and subharmonic motions, this "bouncing ball" system can exhibit large families of non-periodic solutions, especially when the excitation frequency is large and the collisions are nearly elastic. The companion problem in which the surface moves with a prescribed random motion has also been considered [3].

With applications to the slackening of mooring lines in marine engineering, Thompson and Ghaffari [4, 5] examined the frequency response of a harmonically forced oscillator in which the stiffness of the support differed for positive and negative displacements. Although the oscillator's motion was piecewise linear in each half of the state space, the stiffness discontinuity associated with the bilinear spring resulted, under some circumstances, in overall complex responses. Impact can be exploited to dissipate vibration energy [6, 7], and the existence, stability and bifurcation of periodic solutions in such "impact vibration absorbers" have been discussed [8, 9].

In addition to these seemingly simple impact systems, repeated collisions can also be relevant to the response of realistic multi-degree-of-freedom structures. A small amount of free play in the joints of a pin connected truss, for instance, can lead to strongly non-linear dynamic behavior. Moon and Li [10] conducted experiments with a truss comprised of 16 bays, and its motion was judged to be chaotic on the basis of the broadband response spectrum that resulted from periodic input. Other mechanical systems which have been shown to exhibit irregular, chaotic behavior are described in reference [11].

In what follows, a single-degree-of-freedom oscillator that can impact a surface with prescribed sinusoidal motion is studied experimentally and analytically. Machine design issues which are relevant to the motivating mechanical systems above are not addressed here, as the present focus is on developing a basic understanding of driven impact processes. Laboratory measurements for the frequency response of an impacting cantilever beam system are discussed first. Excitation of the oscillator occurs exclusively through its collisions with the surface, and not through a continuously impressed force. In the model, the response between impacts is readily determined because the oscillator is in free vibration during those time intervals, and these piecewise solutions then are subject to juncture conditions which are applied across each impact. In this manner, a non-linear recurrence relation is derived, providing an efficient means by which the forced response can be predicted. Despite the apparent simplicity of the impact oscillator, its behavior under periodic excitation can nevertheless be complicated. Finally, two approximations, which have been made in the modelling of related impact systems, are re-examined here in the light of the experimental results.

2. RESPONSE MEASUREMENTS

Experiments were conducted with the test apparatus shown in Figure 1. A stainless steel strip, 150 mm long, was clamped at one end, and two rectangular blocks were bolted on either side of the beam's free end. A ball bearing was welded to a threaded rod, which in turn was mounted on the platen of a voice coil shaker. This fixture provided a smooth, rounded surface against which the beam could impact, and a sensibly "point" contact. To reduce the acoustic noise that was generated during the experiments and to protect the surface of the beam, a 0·15 mm thick piece of compliant electrical tape was placed on the beam at the point of contact. The tape was replaced periodically to ensure uniformity of the surface. This assembly was not preloaded, so that in the equilibrium state, the beam and shaker were in near contact. The shaker was driven sinusoidally at the specified frequency f and amplitude s_{max}, where its motion was measured with an available accelerometer. An eddy current probe with a linear range of approximately 1 mm was used

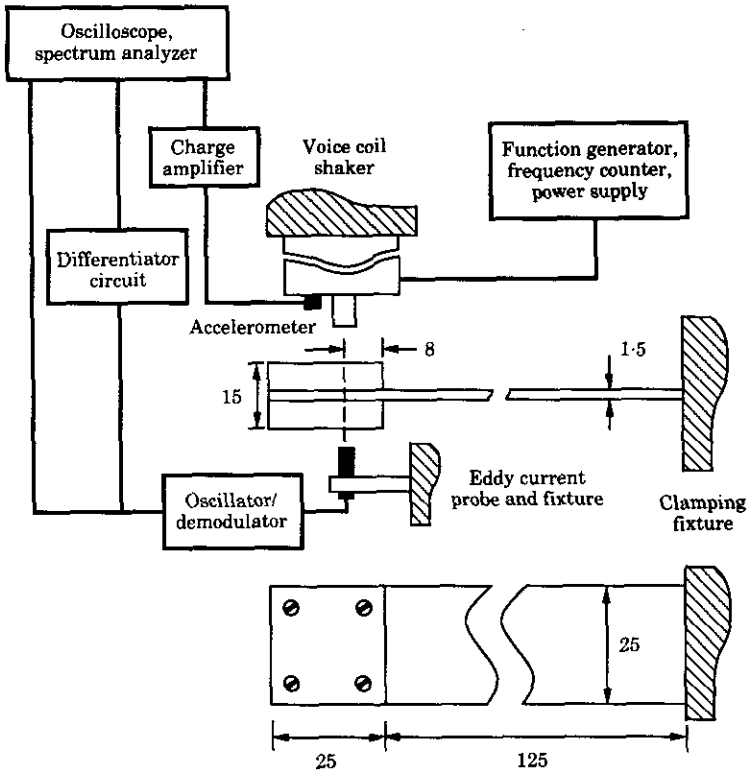

Figure 1. A schematic of the experimental apparatus. The stainless steel cantilever beam with end mass can contact the voice coil shaker which is driven with a prescribed harmonic motion. The dimensions are given in millimeters.

to measure the displacement x of the beam's tip without direct physical contact. A standard active analog differentiation circuit provided the velocity signal $v = \dot{x}$. A 750 Hz low-pass filter reduced the noise generated by the differentiation process, while still preserving the low-frequency signal content which is of relevance here. Time records and x–v state space trajectories were recorded on an analog/digital storage oscilloscope, and a multi-channel spectrum analyzer was available to characterize both the excitation and response signals.

To the extent that multiple vibration modes could be excited during the beam–shaker impacts, one issue of concern was whether the higher vibration modes would dominate the observed motion and mask the non-linear phenomena which are of primary interest. In that regard, transfer functions for the beam were measured with an instrumented force hammer to identify the modes that were excited upon impact. The excitation and measurement points were collocated on opposite sides of the beam, and the displacement probe was mounted on a three-axis translation stage so that its position relative to the beam's tip could be adjusted. With the contact point at the centroid of the blocks, the first three vibration modes contributed to the impulse response in the frequency range 0–400 Hz, as shown in Figure 2(a). By locating the contact point 4·5 mm off-center along the axis of the beam, namely at a point found by cut-and-try to be an approximate node of the second and third vibration modes at 249 and 275 Hz, respectively, the response was dominated by the fundamental mode. This off-center point, indicated in Figure 2(b), was used for all subsequent measurements. The corresponding natural frequency $f_n = 22{\cdot}5$ Hz

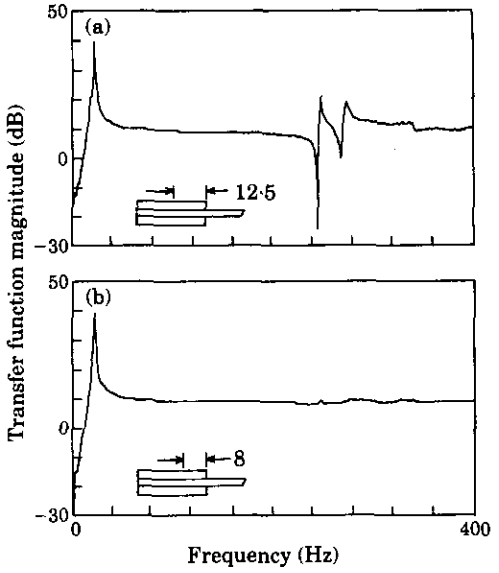

Figure 2. Magnitudes of measured transfer functions. The impact and measurement points were collocated (a) at the center of the end mass, and (b) at an off-center point which is an approximate node of the second and third vibration modes. The first peak occurs at 22·5 Hz.

of the oscillator agrees with the estimate of 25 Hz obtained from

$$f_n = \frac{1}{2\pi}\sqrt{\frac{3EI}{[m + (33/140)m_b]L^3}}, \tag{1}$$

as given by Bishop and Johnson [12]. In this rough calculation, the system was idealized as a cantilever Euler–Bernoulli beam of length L, and flexural stiffness EI, with a concentrated mass m at the free end. For the dimensions specified in Figure 1, the mass ratio m/m_b is approximately 2:1, where m_b is the mass of the beam proper. Note that in the derivation of equation (1), the rotational inertia of m is neglected, and the transverse deformation of the beam is approximated in the Rayleigh–Ritz sense by its static deflection profile, each tending to overestimate f_n. A more detailed model could be used, but this was judged to be unnecessary for the purpose of interpreting the measurement.

The system's response for a specified excitation frequency was characterized by measuring time records for the motions of the shaker's platen (the "surface") and of the beam with end mass (the "oscillator"), frequency spectra for the surface and oscillator, and state space trajectories for the oscillator. The objective of these frequency response tests was to determine the ranges of excitation frequency where the response was periodic (although not necessary with the same period as the excitation), and where it was non-periodic (notwithstanding the system and excitation being deterministic). Measured results at the excitation frequency of 50 Hz are shown in Figure 3. In Figure 3(a), five cycles of the surface's acceleration, and of the oscillator's displacement, are shown in order to indicate the degree of repeatability for the measurements. The oscillator and surface collided once per cycle of the surface's motion, and the response waveform was essentially a rectified sinusoid. The maximum displacement x_{max}, namely the "cusp-to-peak" distance in the oscillator's time record, was 0·29 mm. Note that a transient, high frequency component in the surface's acceleration record occurred immediately after each impact. This "ringing" derived from the repeated reflection of longitudinal waves along the axis of the rod against which the oscillator impacted. As indicated by the spectra shown in

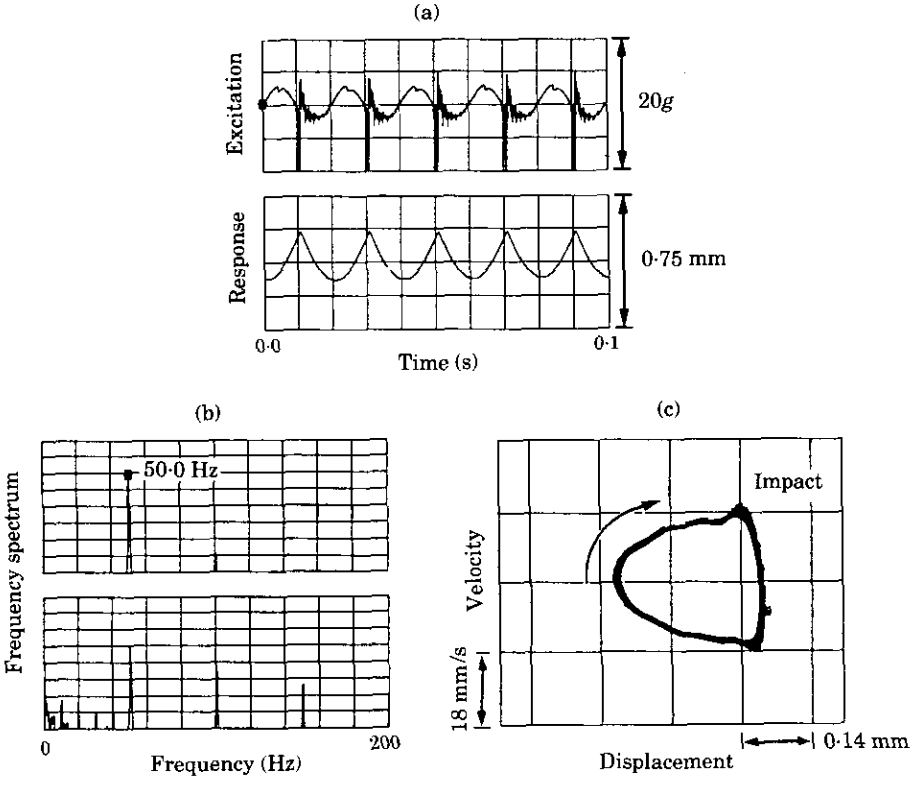

Figure 3. Measured (a) time records, (b) frequency spectra and (c) state space orbits for $f = 50$ Hz (first excitation range), where the response is period-one. In (b), each vertical hashmark corresponds to 10 dB.

Figure 3, the periods of the response and excitation are identical, so that this response is a period-one motion. The oscillator's measured x–v trajectory is also shown in Figure 3 for approximately 25 clockwise cycles. The near-vertical portion of the orbit corresponds to the sudden velocity change which is expected at each impact.

When the excitation frequency was increased to 50·25 Hz, a change of only 0·5%, the qualitative character of the response changed suddenly as depicted in Figure 4. The oscillator continued to contact the surface once per cycle of excitation, but now twice per cycle of response; this is termed a period-two motion. In the oscillator's time record, the amplitudes of the two half-sine waves are 0·21 mm and 0·32 mm. Notably, these values bracket the amplitude in Figure 3 immediately preceding the point of bifurcation. The subharmonic character of the oscillator's behavior is further borne out by the fundamental frequency component in its response spectrum, which occurs at exactly half the excitation frequency. The state space diagram of Figure 4, which again shows approximately 25 complete cycles of vibration, demonstrates that the two impacts during each response cycle occurred at approximately the same value of the oscillator's (or equivalently, the surface's) displacement. The velocity changes associated with the two impacts, however, differed in magnitude by approximately 25%.

As the excitation frequency was increased, the oscillator responded in an apparently random manner within the frequency window of 54–59 Hz. This pattern of periodicity, bifurcation and irregular vibration repeated itself for larger values of f. Measurements taken at 101 Hz, within the second such window of irregular motion, are shown in Figure 5. The ensemble of time records for the oscillator spans approximately 40 cycles of excitation,

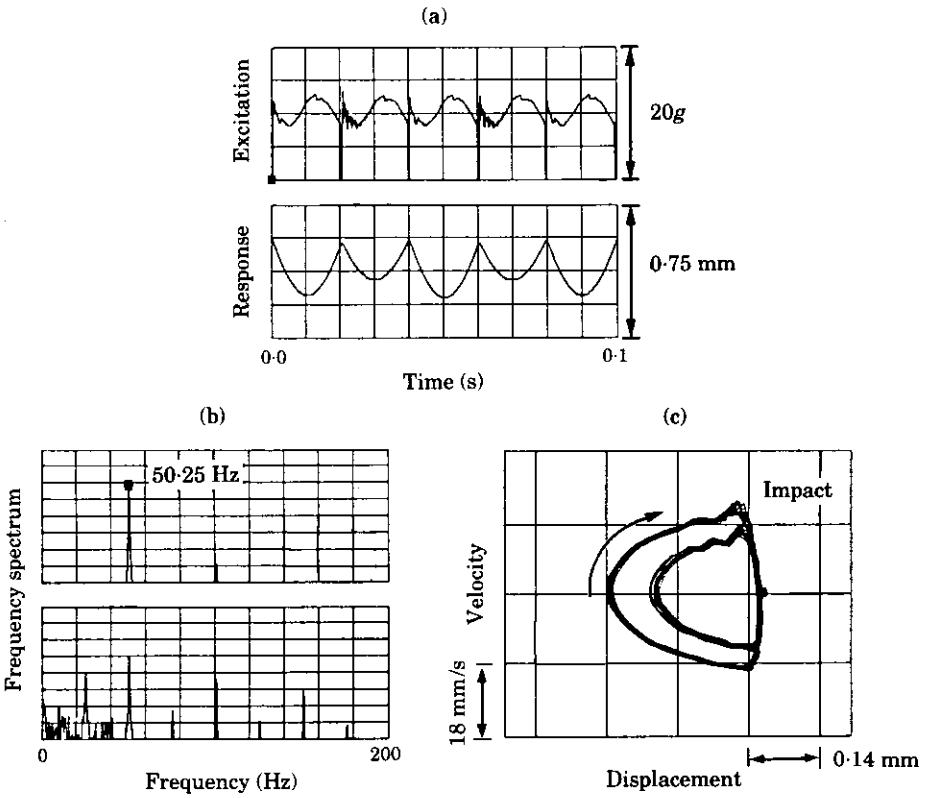

Figure 4. Measured (a) time records, (b) frequency spectra and (c) state space orbits for $f = 50{\cdot}25$ Hz (first excitation range), where immediately following bifurcation the response is period-two. Same scales as Figure 3.

and no apparent periodicity is indicated. The sharp spectral peaks which are evident in the response spectra given in Figures 3 and 4 have been smeared here into a broadband, as is characteristic of chaotic dynamic systems. Although there is a harmonic component to the oscillator's motion at 101 Hz, most of the response energy is localized within the 0–60 Hz band. The state space trajectory in Figure 5 is shown for approximately 50 orbits. Successive impacts between the oscillator and the surface typically occurred at different (positive) displacement values, and the velocity jumps did not have uniform magnitudes. The response of the oscillator remained irregular and apparently non-periodic for the duration of the test.

The compilation of these measurements, and others that were made at excitation frequencies between approximately one and five times f_n, is given in Figure 6. The normalized amplitude of response x_{max}/s_{max} is shown on the ordinate. Regions of irregular response are shaded, and the multiple data points, which are shown for a particular excitation frequency, correspond to the distinct amplitudes of a subharmonic response. Thus, following Figure 4, two data points are shown at $f = 50{\cdot}25$ Hz. Within the frequency window 28 Hz $< f <$ 34 Hz, the oscillator responded in a period-two subharmonic motion, with bifurcation at 28 Hz and subsequent coalescence to a period-one solution at 34 Hz. With f being gradually increased, the amplitude of the period-one motion grew until local resonance was reached at $f = 45$ Hz. Notably, this is approximately twice the oscillator's natural frequency. Just above 50 Hz, the response bifurcated to the period-two motion, as illustrated in Figure 4. Subharmonic motions of order greater than two were not

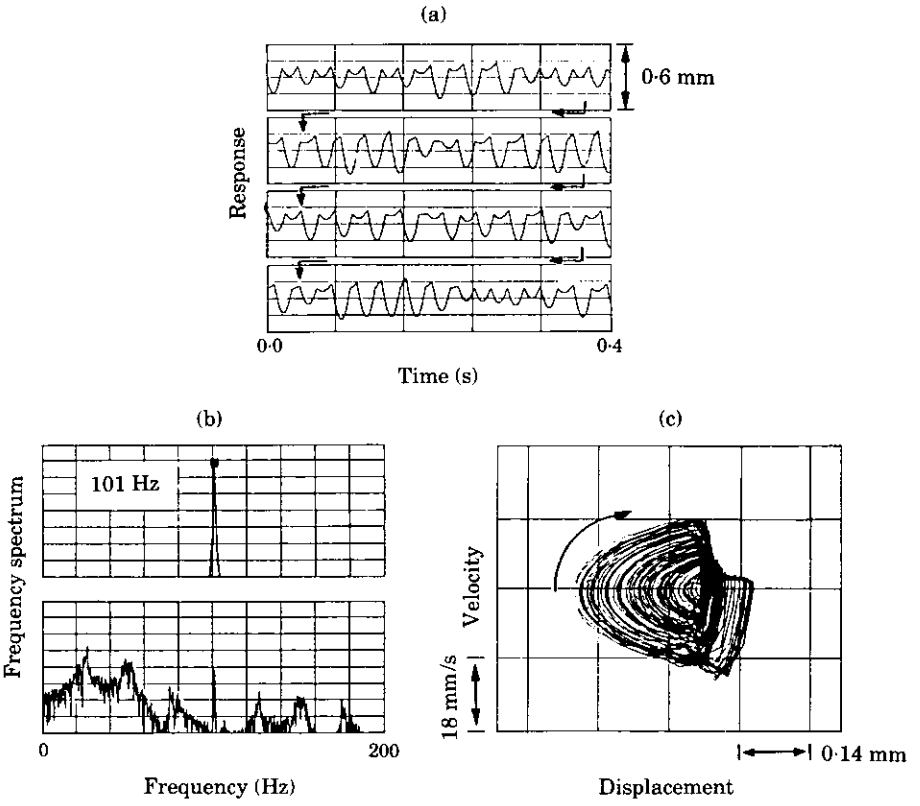

Figure 5. Measured (a) time records, (b) frequency spectra and (c) state space orbits for $f = 101$ Hz (second excitation range), in the window of irregular response. In (b), each vertical hashmark correspond to 10 dB.

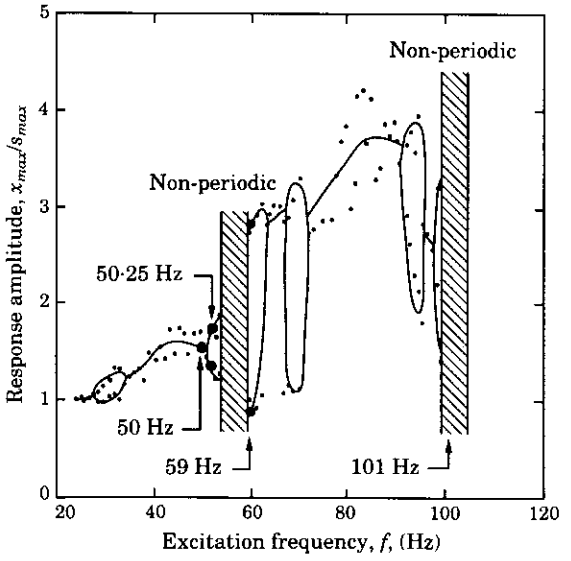

Figure 6. Measured response amplitude in the first two excitation ranges. The motions depicted in Figures 3–5 and in Figure 9 are denoted by the bold data points (●).

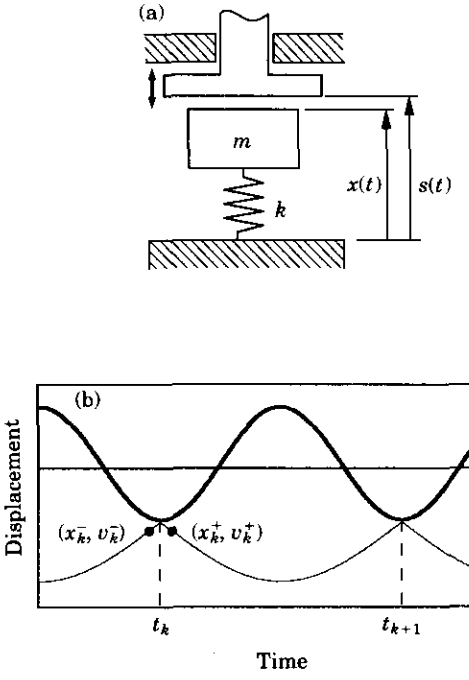

Figure 7. (a) A model of the single-degree-of-freedom oscillator that can contact a surface with prescribed motion, and (b) A schematic illustration of a period-one response. ——, Surface; ——, oscillator.

experimentally observed prior to the first region of irregular motion, although the model that is described below does predict a classic period-doubling cascade. For still larger excitation frequencies, the pattern of (1) resonance of a periodic solution, (2) bifurcation and (3) irregular vibration recurred. In particular, near an even integer multiple of f_n, the amplitude of the periodic response reached a local maximum, and near an odd integer multiple, the motion exhibited period-doubling and apparently non-periodic behavior. With the frequency interval $(2i-1)f_n < f < (2i+1)f_n$, $i = 1, 2, \ldots$, denoted as the ith excitation range, the qualitative character of the observed response is similar over each range, given that the periodic solution at $f \approx 2if_n$ corresponds to i cycles of the surface's motion.

3. MODEL AND IMPLICIT RECURRENCE RELATION

A basic model of the impact system is shown in Figure 7(a). The single-degree-of-freedom oscillator can impact the rigid surface with prescribed motion $s = s_{max} \sin(\omega t)$, where $\omega = 2\pi f$. Motion of the surface is specified to be unaffected by its collisions with m. The displacement x of the oscillator is measured from its rest position, where the spring k is unstretched and the oscillator and surface are in near contact. Impact occurs when $x = s$, and impenetrability of the surface requires that $x \leqslant s$. Dissipation in the oscillator by itself is neglected on the basis of the small measured damping ratio of about 0·3% in the test apparatus. However, energy can be dissipated during impact. The specifics of this complex process are not addressed here and, instead, impact is approximated by the coefficient of restitution $e \leqslant 1$. Although e is frequently considered to be constant for a specified pair of contacting surfaces, in practice it depends on the relative velocity at collision and approaches unity as the velocity tends to zero.

The oscillator is driven by the intermittent impacts associated with motion of the surface. Between impacts, no externally applied force acts on m, so that the free response solution is available for those time intervals. A non-linear recurrence relation is derived such that given the time t_k of the kth impact, and the displacement x_k^+ and velocity v_k^+ of the oscillator immediately afterwards, the state of the oscillator at the instant following the next impact at t_{k+1} can be obtained, as depicted in Figure 7(b). In this manner, the response of the oscillator can be systematically advanced in time, without the computational burden that is associated with direct integration of the oscillator's equation of motion over the (potentially long) time period which is necessary for the system to reach steady state.

The model is non-dimensionalized in terms of the quantities

$$x^* = x/s_{max}, \qquad s^* = s/s_{max}, \qquad t^* = \omega_n t, \qquad \omega^* = \omega/\omega_n, \tag{2}$$

where $\omega_n^2 = k/m$. After henceforth omitting the asterisk notation for convenience, the state vector for the oscillator immediately following the kth impact is

$$\mathbf{x}_k^+ = \begin{Bmatrix} x_k^+ \\ v_k^+ \end{Bmatrix}. \tag{3}$$

Motion of the oscillator over $t \in (t_k^+, t_{k+1}^-)$ satisfies $\ddot{x} + \omega_n^2 x = 0$, where the displacement and velocity during this free vibration interval are

$$\begin{aligned} x(t) &= x_k^+ \cos(t - t_k) + v_k^+ \sin(t - t_k), \\ v(t) &= -x_k^+ \sin(t - t_k) + v_k^+ \cos(t - t_k). \end{aligned} \tag{4}$$

The time t_{k+1} at which the next impact occurs is therefore the first root of

$$\sqrt{(x_k^+)^2 + (v_k^+)^2}\sin((t_{k+1} - t_k) + \tan^{-1}(x_k^+/v_k^+)) - \sin(\omega t_{k+1}) = 0, \tag{5}$$

and substitution in equation (4) provides the state of the oscillator

$$\mathbf{x}_{k+1}^- = \begin{bmatrix} \cos(t_{k+1} - t_k) & \sin(t_{k+1} - t_k) \\ -\sin(t_{k+1} - t_k) & \cos(t_{k+1} - t_k) \end{bmatrix} \mathbf{x}_k^+ \tag{6}$$

at the instant before t_{k+1}. The states at t_{k+1}^+ and t_{k+1}^- are related by continuity of displacement, namely that $x_{k+1}^+ = x_{k+1}^-$, and by the velocity change

$$v_{k+1}^+ = -ev_{k+1}^- + (1 + e)\omega \cos(\omega t_{k+1}). \tag{7}$$

In this manner, the oscillator's state vector is advanced across the impact by the inhomogeneous relation

$$\mathbf{x}_{k+1}^+ = \begin{bmatrix} 1 & 0 \\ 0 & -e \end{bmatrix} \mathbf{x}_{k+1}^- + \begin{Bmatrix} 0 \\ (1 + e)\omega \cos(\omega t_{k+1}) \end{Bmatrix}. \tag{8}$$

To numerically simulate the response through this procedure, initial values for the displacement and velocity are specified, and equation (5) is solved to determine the time at which the first collision with the surface occurs. Roots of equation (5) are found by using a combination of the Newton–Raphson and bisection methods. The state vector (3) is advanced across the free vibration interval by equation (6), and then across the impact through equation (8). This process is repeated recursively to determine the second time of impact, and so forth. Time records of the oscillator's motion, spectra and x–v trajectories can be reconstructed from equation (4) and from the stored values of t_k and $\mathbf{x}_k^+$. Solutions obtained in this manner have been verified by comparison to the results from direct numerical integration of the oscillator's equation of motion with an adaptive Fehlberg

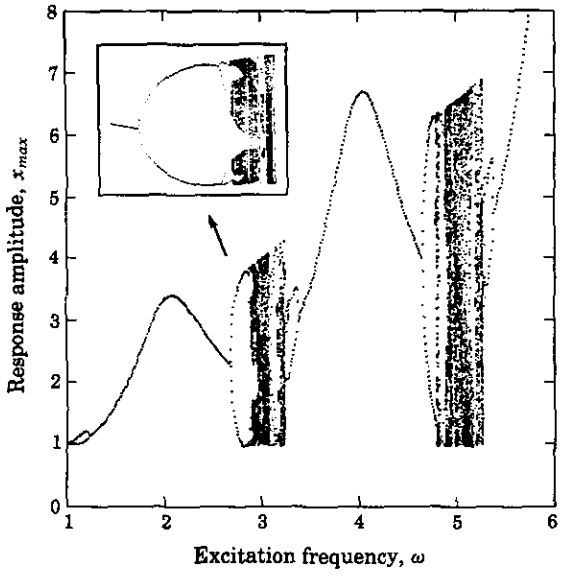

Figure 8. The predicted frequency response of the model for $e = 0{\cdot}4$. The dimensionless cusp-to-peak vibration amplitude x_{max} is shown on the ordinate.

fourth/fifth order Runge–Kutta algorithm [13]. Note that in numerical integration, as equation (5) of the recurrence relation, it is important to accurately determine the times of impact.

A predicted frequency response diagram with $e = 0{\cdot}4$ is shown in Figure 8 for $\omega_n < \omega < 6\omega_n$. The inset details the behavior near transition between the period-two and period-four solutions in the first excitation range. As above, local resonance of the periodic solutions occurs when $\omega \approx 2i$, $i = 1, 2, \ldots$ Similarly, period-doubling bifurcations and irregular motion occur for $\omega \approx 2i - 1$. Note that the incomplete "Feigenbaum tree" immediately above $\omega = 1$ was recorded in the measurements. Based on the overall structure of the response diagram, the predictions of the model agree with the experimental observations, although the model does consistently overestimate the vibration amplitude. This discrepancy could be due to the choice of the coefficient of restitution in Figure 8, as there was substantial scatter in the measured values, which ranged between approximately 0·3 and 0·5, for the test apparatus.

4. DISCUSSION

The present solution technique does not involve two approximations that have been made in studies of related impact systems [2, 3]. First, in the model, the surface can have prescribed motion of arbitrarily large amplitude, and in particular, the restriction $x_{max} \gg s_{max}$ is not imposed. Through non-dimensionalization in equation (2), the physical amplitude of the surface's motion is scaled out, and s_{max} does not appear explicitly in the subsequent development. For this reason, the predicted physical response is directly proportional to the amplitude of the surface's motion. This is an interesting property of the impact oscillator, which is derived from its piecewise linear character and which simplifies the description of its non-linear response. The approximation $x_{max} \gg s_{max}$ is appropriate for high frequency excitation, where the velocity of the surface is large, and in particular near $\omega \approx 2i$, where a periodic solution experiences resonance. The approxi-

mation is problematic for the impact system considered here when $\mathcal{O}(x_{max}/s_{max}) = 1$ in either Figure 6 or Figure 8. Furthermore, in the frequency windows where irregular motion occurs, the amplitude of the oscillator changes with time and does not necessarily always satisfy the assumption that $x_{max} \gg s_{max}$. However, when the motion of the surface has a sensibly small amplitude, equation (5) provides the approximate time of impact

$$t_{k+1} \approx t_k - \tan^{-1}(x_k^+/v_k^+) + \pi. \tag{9}$$

Substitution in equations (6) and (8) provides an explicit recurrence relation for the oscillator's state, which can be implemented and analyzed more easily than the implicit numerical procedure which is used here.

As a second modelling issue, when the above recurrence technique is used, the oscillator need not reverse its direction upon impact with the surface: namely, the restriction $(v_{k+1}^+)(v_{k+1}^-) < 0$ is not imposed. In fact, motions which do not involve velocity reversal upon impact were observed experimentally as illustrated in Figures 9(a) and 9(b). There, the depicted motion is periodic with two impacts per response cycle. The impacts occur in rapid succession, and only one is direction reversing. The corresponding orbit which is predicted by the model is shown in Figure 9(c). The direction of the oscillator's motion remains unchanged across one of the two impacts, and the "+" and "−" signs which are shown indicate the sign of the velocity before and after each impact. Furthermore, impacts without velocity reversal were also observed in Figure 5 for non-periodic motion. In short, although the recurrence technique used here is complicated by the implicit nature of equation (5), the method is capable of predicting responses which are not allowed by a simpler direction-reversing mapping. Similar observations have been made in the analysis of a related impacting system [14].

In Figure 10, Poincaré sections, each containing 10 000 points, are shown at phase increments of 5% of one complete excitation cycle. The phase space projections comprise three "leaves" with narrow "stems" that extend radially outward. The fractal-like structure of the section suggests a chaotic solution. As the excitation phase increases from zero to

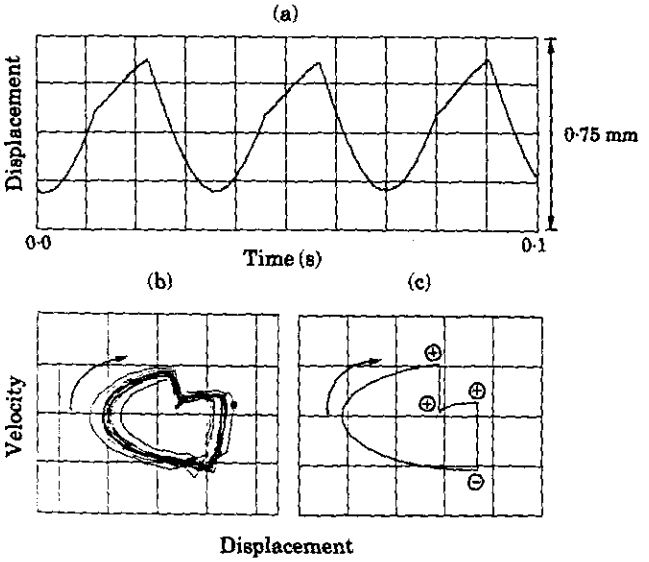

Figure 9. The periodic motion of the oscillator in which two collisions occur in rapid succession. (a) The measured time record at 59 Hz; (b) the measured state space trajectory; (c) the predicted trajectory, where the sense of the velocity before and after each collision is indicated.

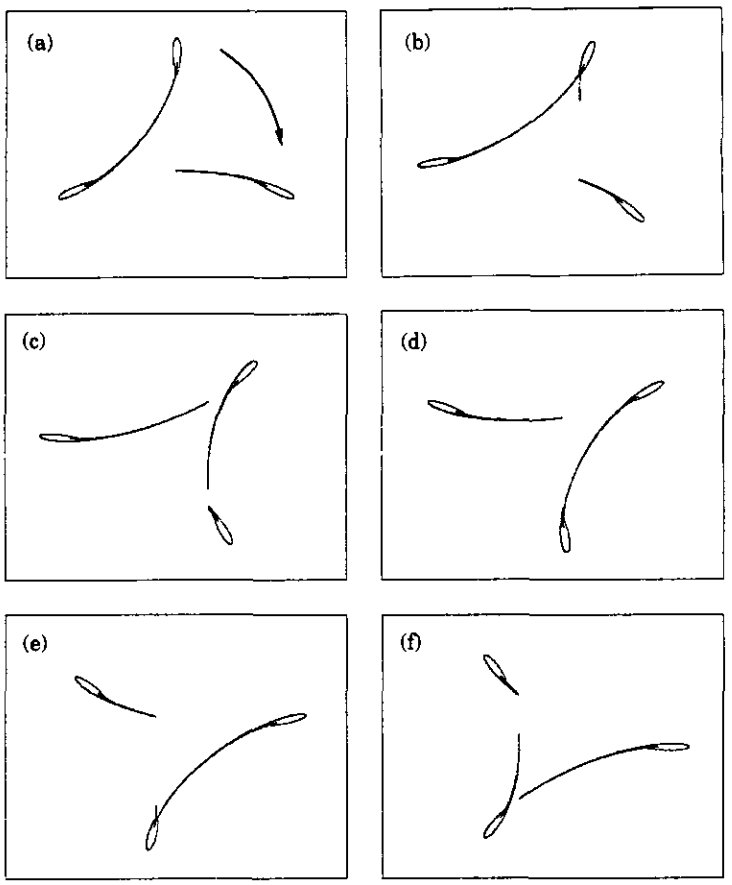

Figure 10. Poincaré sections at $\omega = 3$ for different phases over the first quarter of the excitation cycle. The non-dimensionalized displacement is shown on the abscissa, and velocity on the ordinate. The sections for the sequence of planes $6\pi/10, \ldots, \pi$ appear similar to those shown: (a) 0; (b) $\pi/10$; (c) $2\pi/10$; (d) $3\pi/10$; (e) $4\pi/10$; (f) $5\pi/10$.

one-quarter of the period, the structure rotates clockwise in Figure 10 by approximately $\pi/2$ radians. Over the subsequent ranges of phase from one-quarter to one-half of the excitation cycle, one-half to three-quarters and so forth, the animated sequence of sections is similar in appearance to Figure 10. Construction of these diagrams for other excitation ranges indicates that, in general, for irregular motion near $\omega = 2i + 1$, there are $2i + 1$ stem-and-leaf pairs.

5. SUMMARY

Measured response time records, frequency spectra and state space trajectories for the driven impact oscillator are compared to results from a non-linear recurrence relation which is derived for the state of the oscillator from one impact to the next. To simplify the form of the state mapping, previous models of related impact processes have specified that the response amplitude is large compared to that of the surface, and that the direction of motion reverses upon each impact. In the present case at least, such a model cannot capture all classes of motion which are observed experimentally, although implementation of the implicit technique is more involved than for a simpler mapping. The amplitude of

the surface's motion is scaled out in non-dimensionalization of the equation of motion, and as a result, the two dimensionless parameters e and ω determine the qualitative character of the response, which can be either periodic or irregular. The criteria used here for classifying the latter chaotic responses are the spectral content of the response under a periodic excitation, the apparent non-repeatability of the state space trajectory, and the structure of the calculated Poincaré sections.

ACKNOWLEDGEMENT

This material is based (in part) upon work supported by the National Science Foundation under Grant Number ECD-8907068. The government has certain rights in this material.

REFERENCES

1. R. N. ARNOLD, G. N. BYCROFT and B. B. WARBURTON 1955 *Journal of Applied Mechanics* **22**, 391–400. Forced vibration of a body on an infinite elastic solid.
2. P. J. HOLMES 1982 *Journal of Sound and Vibration* **84**, 173–189. The dynamics of repeated impacts with a sinusoidally vibrating table.
3. L. A. WOOD and K. P. BYRNE 1981 *Journal of Sound and Vibration* **78**, 329–345. Analysis of a random repeated impact process.
4. J. M. T. THOMPSON and R. GHAFFARI 1982 *Physics Letters* **91A**, 5–8. Chaos after period-doubling bifurcations in the resonance of an impact oscillator.
5. J. M. T. THOMPSON and R. GHAFFARI 1983 *Physical Review* **27A**, 1741–1743. Chaotic dynamics of an impact oscillator.
6. J. SHAW and S. W. SHAW 1989 *Journal of Applied Mechanics* **56**, 168–174. The onset of chaos in a two-degree-of-freedom impacting system.
7. C. N. BAPAT and S. SANKAR 1985 *Journal of Sound and Vibration* **99**, 85–94. Single unit impact damper in free and forced vibration.
8. S. F. MASRI and T. K. CAUGHEY 1966 *Journal of Applied Mechanics* **33**, 586–592. On the stability of the impact damper.
9. N. POPPLEWELL, C. N. BAPAT and K. MCLACHLAN 1983 *Journal of Sound and Vibration* **87**, 41–59. Stable periodic vibroimpacts of an oscillator.
10. F. C. MOON and G. X. LI 1990 *American Institute of Aeronautics and Astronautics Journal* **28**, 915–921. Experimental study of chaotic vibrations in a pin-jointed space truss structure.
11. F. C. MOON 1987 *Chaotic Vibrations*. New York: John Wiley.
12. R. E. D. BISHOP and D. C. JOHNSON 1960 *The Mechanics of Vibration*. Cambridge: Cambridge University Press.
13. G. E. FORSYTHE, M. A. MALCOLM and C. B. MOLER 1977 *Computer Methods for Mathematical Computations*. Englewood Cliffs, New Jersey: Prentice-Hall.
14. C. N. BAPAT, S. SANKAR and N. POPPLEWELL 1986 *Journal of Sound and Vibration* **108**, 99–115. Repeated impacts on a sinusoidally vibrating table reappraised.